THE PHOTOGRAMMETRIC RECORD

The Photogrammetric Record 28(141): 96–114 (March 2013)
DOI: 10.1111/j.1477-9730.2012.00704.x

ACCURACY ASSESSMENT OF COMMERCIAL SELF-CALIBRATING BUNDLE ADJUSTMENT ROUTINES APPLIED TO ARCHIVAL AERIAL PHOTOGRAPHY

Manuel A. Aguilar (maguilar@ual.es)
Fernando J. Aguilar (faguilar@ual.es)
Ismael Fernández (ismaelf@ual.es)
University of Almería, Spain

Jon P. Mills (jon.mills@ncl.ac.uk)
Newcastle University, UK

Abstract

The use of archival or historical photography for photogrammetric purposes often involves a lack of data concerning the aerial cameras employed, difficulties in identifying control points on the photos and inappropriate conservation of the photography. When camera calibration parameters are unknown, they should be estimated by means of a self-calibrating bundle adjustment. Several calibration models available in the Leica Photogrammetry Suite software have been tested on two archival datasets, captured in 1956 and 1977, covering the same working area. The accuracy of the dataset triangulation was found to depend significantly on the self-calibration method and the number of ground control points used; when the latter ranged from six to nine per stereopair, self-calibrating bundle adjustment techniques were found to slightly, but not always significantly, improve the photogrammetric capability of archival aerial photography. Thus, the adoption of self-calibration cannot guarantee the improvement of results when working on poorly conserved imagery. Results from such datasets are very dependent on numerous local variables which cannot be extrapolated to other areas for the same camera since each dataset is unique and may present systematic errors of a different nature.

Keywords: accuracy, archival photography, bundle adjustment, mapping, self-calibration, triangulation

Introduction

Archived aerial photography is currently receiving the attention of many earth scientists, with such datasets representing a very important information source in order to evaluate the temporal spatial evolution of zones of interest. Aerial photographs are the earliest remote sensing data source, having being collected since the early 20th century, and photogrammetric and digital image processing techniques are now being extensively used to extract both qualitative and quantitative information from such datasets. Appropriate comparison of photogrammetric surveys of an area conducted in different years allows the identification of accurate geometric change over time. Such techniques have been successfully applied to detect changes in glaciated areas (Schiefer and Gilbert, 2007), riverbank erosion (Lane, 2000), coastal evolution (Mills et al., 2005), gully erosion (Marzolff and Poesen, 2009), forest canopy cover (Véga and St-Onge, 2008) and landslides (Chadwick et al., 2005; Prokešová et al., 2010).

Metric aerial photography has been routinely collected in North America and Europe for land surveying and topographic purposes over the past 50 years or so. However, significant problems can present themselves when attempting to make metrical use of archival aerial photography. For example, the proper conservation of the original film, derived diapositives or prints is not readily guaranteed, and there is often a critical lack of information with respect to the cameras employed, in particular, the regular absence of a geometric calibration certificate. Another general problem when utilising archival photography for metric purposes is the difficulty in locating sufficient ground control points (GCPs), both in terms of quantity and quality, because often the suitable potential points that can be identified in the archival images can no longer be located on the ground at the present time (Zanutta et al., 2006; Walstra et al., 2007).

When camera calibration parameters are unknown (the most usual case when working with archival photography), then they should be estimated using a self-calibrating bundle adjustment (for example, Chandler and Cooper, 1989; Kraus, 1997). Self-calibration is a well-known method which has long been successfully and routinely applied in close range photogrammetric applications utilising non-metric cameras (Fraser, 1997). In recent years, self-calibration has also been increasingly applied in aerial photogrammetry. In fact, most current digital photogrammetric workstations incorporate triangulation software which offers self-calibration options. Among them are the self-calibration routines which use additional parameters (APs) in the triangulation process, as available in the advanced options within the aerial triangulation module of the Leica Photogrammetry Suite (LPS) software. Self-calibration methods were intensively researched and developed in the 1970s and 1980s, where it was confirmed that systematic image errors can be completely or partially compensated by APs (Bauer and Müller, 1972; Ebner, 1976; Grün, 1978; Klein, 1979; Ackermann, 1981). Nowadays, such approaches are routinely used for improving the triangulation process with modern airborne digital sensors such as the ADS40/80 by Leica Geosystems, DMC by Z/I Imaging or UltraCAM by Microsoft/Vexcel Imaging (see, for example, Cramer, 2009). Moreover, other applications are arising using these methods such as the calibration of panoramic cameras and laser scanners (Amiri Parian and Gruen, 2010; Lichti, 2010). The successful application of self-calibration depends on many factors which include: the strength of the block (fore-and-aft overlap, cross-strips); the number and distribution of GCPs and tie points; the magnitude of any systematic errors present; and the significance of, and correlation between, the APs used. In order to extract high-quality data from archival aerial photography, where there may be only a small number of images available and the redundancy may be low, GCPs should be of high quality and well distributed in the block. This is especially important if camera calibration information is incomplete or unavailable. However, the identification and quality of ground control in archival photography is often problematic. As a result, much research has been carried out in order to reduce the need for these costly and difficult to measure GCPs by means of surface matching (see, for example, Li et al., 2001; Mills et al., 2003, 2005; Miller et al., 2008; Akca, 2010; Aguilar et al., 2012), or extracting GCPs from lidar-derived digital elevation models (DEMs) (James et al., 2006).

Nowadays the results regarding the application of self-calibration to archival photography are extremely variable. Firstly, it cannot be assumed that systematic image errors are constant for the entire archive of photographs; every archival flight will present its own systematic errors depending on the camera used, the image scale and so on. Secondly, due to a usual lack of existing ground points, accuracy reports are usually based on an insufficient number of independent check points (CPs), producing low reliability for the accuracy assessment. Finally, replication of the experiments (repetition of the experimental conditions so that the variability associated with the phenomenon can be estimated) is hardly ever undertaken.

This work is part of a large programme of research investigating the monitoring and modelling of the evolution and vulnerability of coastal areas. In that research project, multisource and multitemporal geospatial data are being integrated in a pilot study area. Within this context, the main objective of the work reported in this paper was therefore to investigate the use of self-calibration models to try to improve the photogrammetric capabilities of two archival aerial flights captured in 1956 (1:33 000 scale) and 1977 (1:18 000) over the specific pilot area. The underlying hypothesis supposes that self-calibrating bundle adjustment techniques will correct the difference between the mathematical model of perspective geometry and the true image geometry for archival aerial photography and so remove, at least partially, any systematic errors present. By using a large number of ground points, a statistical analysis to determine the influence of various factors on the accuracy of triangulating these specific archival photographic datasets was performed. The factors considered and reported herein were: (i) the different models utilised in self-calibrating bundle adjustment available in the LPS 9·1® software (models of Bauer, Jacobsen, Ebner, Brown and lens distortion); and (ii) the number of GCPs used in the triangulation process.

STUDY SITE, DATASETS AND METHODOLOGY

Study Site

The study area comprises the heavily developed coastal fringe of Almería, bordering the Mediterranean Sea in Southern Spain, approximately 11 km long and 775 m wide. The working area is situated between the harbours of Garrucha and Villaricos (Fig. 1), and is centred on the WGS 84 coordinates of 605 870 m E, 4 119 869 m N. The intense urbanisation of this coastal fringe during the last 50 years has provoked significant changes in its landscape and induced serious natural disasters, for example, the loss of a strip of shore approximately 200 m wide at Quitapellejos Beach (Palomares).

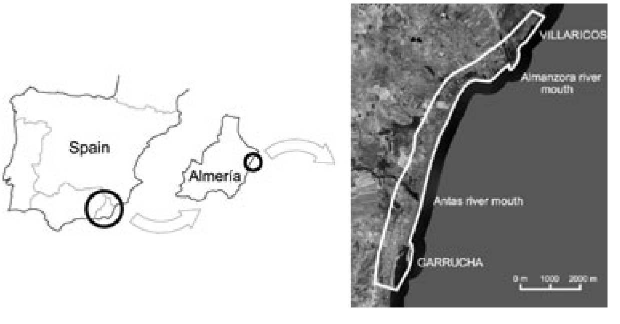

FIG. 1. Location of the study site on the Almerían coast, Spain.

TABLE I. Main characteristics of the analysed archival photogrammetric datasets.

Date	*Number of images*	*Scale*	*Flying height (m)*	*Principal distance (mm)*	*Scan resolution (μm)*	*GSD (m)*	*Image type*	*DGPS/SP ground points measured*
1956	4	1:33 000	5650	154·19 / 153·01	21	0·70	B/W	86 h/84 v
1977	8	1:18 000	2980	152·77	15	0·27	B/W	89 h/77 v

GSD: ground sample distance; DGPS: differential global positioning system; SP: stereophotogrammetry. Ground points: horizontal (h) and vertical (v).

Datasets

1956 Dataset. The 1956 photography was the first of the two archival datasets, both acquired using a "standard" metric film camera format of 230 mm × 230 mm, used in this study (Table I). From a historic perspective, although the systematic flights from 1945 to 1946 were apparently the first photogrammetric project covering most of Spanish territory (Quirós and Fernández, 1997), the 1956 dataset is probably the oldest covering Almería, the study site of this paper. Undertaken by the US government, it is often referred to in Spain as the "American flight" and in most regions of the country marks the start of the archival record of metric aerial photography. It is therefore regarded as a valuable national information source for photo interpretation and land use evolution.

As shown in Fig. 2, four photographs from this dataset were required to cover the entire study area. These photographs belonged to panchromatic photogrammetric flights at an approximate scale of 1:33 000, with 60% forward overlap and 30% lateral overlap, providing a base-to-height (B/H) ratio of approximately 0·60. The original negatives were scanned using a photogrammetric scanner with a geometric resolution of 21 μm and a radiometric resolution of 8 bits; they were stored in TIFF format giving a ground sample distance (GSD) of approximately 0·70 m. The digitised photographs were provided by the Network of Environmental Information of Andalusia (known as REDIAM).

The southern stereopair was captured on 30th October 1956, using a photogrammetric camera for which the principal distance (153·01 mm) appeared as marginal data in the imagery. The northern stereopair was taken on 3rd September 1956, using a different camera with an indicated principal distance of 154·19 mm. Full camera calibration details of these cameras were unknown. Moreover, these old cameras had no corner fiducial marks, as more recent cameras do. Instead, they relied on only four marks in the middle of the edges of the photo frames to allow for interior orientation in the plate carriers of analogue stereoplotters of the time.

1977 Dataset. The 1977 dataset consisted of a panchromatic analogue photogrammetric flight that is commonly referred to in Spain as the "agriculture photogrammetric flight". Four stereopairs from this survey, with a B/H ratio of 0·55, were used to cover the study area (Fig. 2), presenting a 60% forward overlap and a 30% lateral overlap, respectively. This flight presented an approximate scale of 1:18 000 and a principal distance, printed as marginal data in the photographs, of 152·77 mm. The camera calibration certificate was unavailable. The eight photographs were scanned into a TIFF format from the original negatives using a photogrammetric scanner with a geometric resolution of 15 μm and 8 bit radiometric resolution, presenting a GSD of approximately 0·27 m. The photography from this flight had four fiducial marks in the corners of the frame.

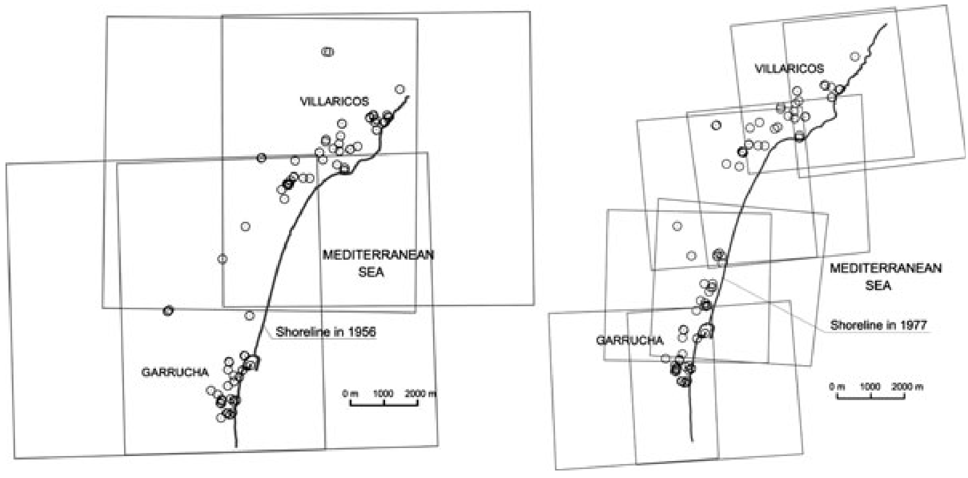

FIG. 2. Configuration scheme for photography, ground points and shoreline in the two archival datasets tested: 1956 (left) and 1977 (right). Note that the coastline position limits the collection of an optimal distribution of GCPs.

2009 Dataset. The final aerial dataset used was flown on 28th August 2009 and consisted of a combined photogrammetric and lidar survey at a flying height above ground of approximately 1000 m. Digital images were obtained using an Intergraph Digital Mapping Camera (DMC), utilising a ground GPS reference station. A total of 86 high-resolution panchromatic images were captured simultaneously with multispectral images in four bands (red, green, blue and near infrared), presenting a composite GSD of approximately 0·10 m. Image orientation was directly measured using a GPS/INS system on board the aircraft which was used to aid the photogrammetric block triangulation. This flight was used to photogrammetrically generate new 3D ground points to be subsequently transferred to the older datasets.

Ground Survey. In conventional aerial surveys, the coordinates of ground points (both GCPs and CPs) are collected at the same time as the photogrammetric survey using topographic surveying techniques. In this case, due to the lack of any such data, man-made and natural points located inside the study area were unambiguously identified in the two archival datasets being assessed. Most ground points were obtained by a differential global positioning system (DGPS) using a Topcon HiPer PRO GOS receiver working in real time kinematic (RTK) mode. The coordinates of 150 ground points, located on well-defined features, were measured with reference to the European Terrestrial Reference System 1989 (ETRS89) and UTM projection. The vertical datum took the geoid as the reference surface, adopting the mean sea level in the calm seas of Alicante, Spain, as the null orthometric height datum. The DGPS observations were supported by 11 survey points: four belonging to the national geodetic network, one obtained using high-precision GPS techniques (Spanish REGENTE network) and six survey points provided by REDIAM. The root mean square errors (RMSE) obtained were 56, 33 and 76 mm in the X, Y and Z axes, respectively.

The task of identifying ground points for the archival datasets was very difficult due to the significant changes in the coastal fringe during the last five decades. It proved especially difficult in the case of the 1956 dataset due to several reasons: it was the oldest photography, the original film was not well preserved and the photographic scale was relatively small. These factors are exemplified in Figs. 3 and 4. As a result of this, of the original 150 survey points, only 47 and 51 DGPS ground points could be used for the 1956 and 1977 flights, respectively. Furthermore, because of the coastal scenes and significant changes in its landscape, the spatial distribution of these ground points was poor. To improve this situation, 45 additional ground points, for which direct access with GPS was very difficult, were observed from the aforementioned 2009 photogrammetric dataset using a SOCET SET® v.5·3 digital photogrammetric workstation by BAE Systems. Of these points, 39 and 38 were finally used in the 1956 and 1977 triangulation projects, respectively. For a number of these points, typically corners of buildings where there was an apparent height change over time, only horizontal coordinates were utilised. The estimated accuracy of the 2009 photogrammetric project, calculated as the three-dimensional root mean square error ($RMSE_{3d}$) on 57 CPs measured by DGPS, was 0·247 m ($RMSE_x$ 0·136 m, $RMSE_y$ 0·123 m and $RMSE_z$ 0·167 m).

Self-Calibrating Bundle Adjustment Models

Five self-calibrating bundle adjustment models were tested on the two historic flights using a variable number of GCPs. These models were compared with bundle adjustments conducted without self-calibration models (subsequently referred to as no self-calibration, NSC). All the photogrammetric projects were carried out using LPS 9·1® software, produced by Leica Geosystems.

The NSC bundle adjustment was applied to both historic datasets. The principal distance and principal point position were held fixed. The principal distance printed as marginal data in the aerial photography was used as the camera calibration information and the principal point was set to $x_0 = 0$ and $y_0 = 0$, so that no offset was assumed between the principal point and the fiducial centre. In order to solve the interior orientation, the photo coordinates for the fiducial marks were required for each camera used. With no fiducial mark information available, the following steps were carried out: (i) a digital photograph at the correct scale was loaded into CAD software; (ii) a translation was computed such that the image coordinates of the point where the lines joining opposite fiducial marks intersected was assigned as the origin (zero) of the photo coordinates; (iii) a rotation was applied to fix the angle between the

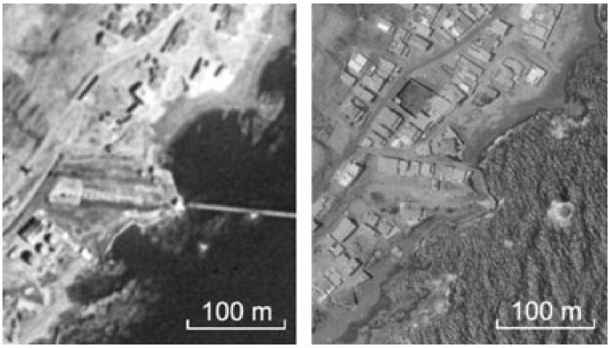

FIG. 3. Coastal village of Villaricos on the 1956 (left) and 1977 (right) photographs.

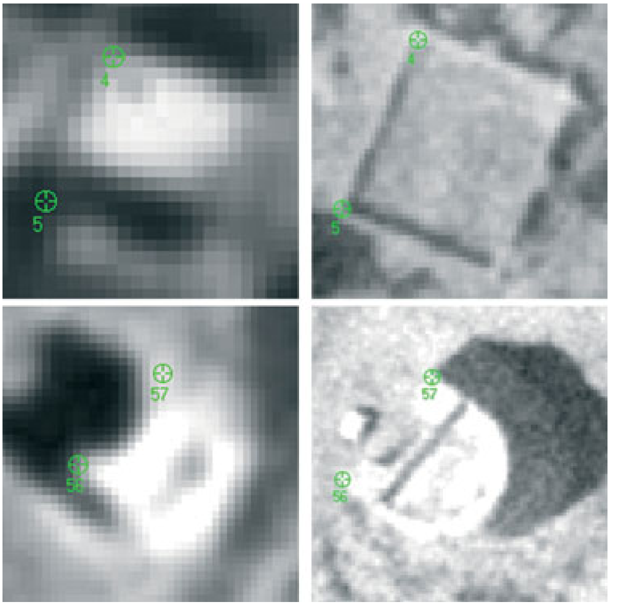

FIG. 4. Ground points marked on the same features as they can be visualised in the 1956 (left) and 1977 (right) photogrammetric datasets tested.

principal point and the first fiducial mark to 0° (in cases where the fiducial marks were only available along the edges of the photo frame) or 45° (where the fiducial marks were placed in the corners of the photo frame); (iv) the image coordinates of the fiducial marks were precisely measured on each digital image using the CAD software; (v) finally, the mean of the fiducial mark coordinates for all the photographs in every dataset were used to compute each camera's interior orientation. Note that for the 1956 dataset two cameras were used, thus two different sets of fiducial marks and principal distance values were entered.

Besides the NSC bundle adjustment triangulation, five other self-calibrating bundle adjustment triangulations (advanced options in the aerial triangulation module of the LPS software) were undertaken. These models are incorporated in the collinearity equations, which allow for the modelling of various systematic errors associated with the camera/sensor model and atmospheric refraction. Five different self-calibrating models can be used in the triangulation process offered by LPS:

(1) *Lens distortion model*. This is designed to self-calibrate the lens distortion parameters automatically. This model has two APs (k_1 and k_2).
(2) *Bauer's simple model*. This has three APs, two parameters determine the extent of affine deformation (non-orthogonality and scale differential between the two axes in space image) and one parameter estimates symmetric lens distortion.
(3) *Jacobsen's simple model*. This has four APs, which compensate for the first- and second-order distortions associated with affine deformation and lens distortion.
(4) *Ebner's orthogonal model*. This model has 12 APs which compensate for various types of systematic error. It mathematically models and eliminates the systematic image errors in the location of the von Gruber points, without any physical background. Since a greater number of parameters are estimated, an increased number of GCPs are required.

(5) *Brown's physical model*. This has 14 APs which compensate for most of the linear and non-linear forms of film and lens distortion.

Further information regarding all models implemented in LPS can be found in the Leica Photogrammetry Suite Project Manager (Leica Geosystems, 2006).

Photogrammetric Projects from the 1956 and 1977 Datasets

Ninety individual photogrammetric experiments were performed using the 1956 dataset. Six triangulation models, both with and without self-calibration models, were tested (NSC, lens distortion, Bauer's, Jacobsen's, Ebner's and Brown's). Three different repetitions of 9, 18, 27, 36 and 45 GCPs, obtained either by DGPS or from the 2009 flight, were extracted from the initial 86 ground points. The 15 sets of GCPs extracted had the best possible distribution, although some weak areas were identified. Once the task of observing every ground point (GCPs and CPs) in the image space was complete (noting that the interior orientation and photo coordinates for each ground point remained constant for every project), the LPS automatic tie point collection was performed. Thus, 44 tie points were automatically generated for the 1956 flight. These were visually checked and manually edited as required. The exterior orientation of each photogrammetric project was then computed. Because any aerial triangulation accuracy assessment should ideally be based upon CPs, in other words those ground points not used in the aerial triangulation process, the remaining ground points were used as CPs for computation of the $RMSE_{3d}$ for each photogrammetric project. The number of CPs therefore ranged from 41 to 77, depending on the number of GCPs employed.

The same methodology was followed for the 1977 dataset. In this way, 90 photogrammetric cases were computed, but in this instance, 89 ground points and 95 tie points were used to compute the bundle adjustment for every photogrammetric block. The 15 groups of GCPs showed a slightly better distribution than in the 1956 case, although there were still zones where new urbanisation meant new ground points could not be measured (Fig. 5).

Statistical Analysis

In order to study the influence of different factors on aerial triangulation accuracy, analysis of variance (ANOVA) tests were utilised. ANOVA is a common statistical tool used to analyse datasets for which the importance of several factors is evaluated at once (Snedecor and Cochran, 1980). In this case, the observed variables in the ANOVA for the designed factorial model with three repetitions were the planimetric RMSE ($RMSE_p$), vertical RMSE ($RMSE_z$) and $RMSE_{3d}$, corresponding to the 1956 and 1977 projects. The sources of variation, or factors, were the number of GCPs, the employed self-calibration method and the cross-interactions between them all. When the results of the ANOVA turned out to be significant, the separation of means was carried out using Duncan's multiple range test at a 95% confidence level.

It is noteworthy that all the residual populations at the *X*, *Y* and *Z* axes were tested for the normality of their distribution by means of the Kolmogorov–Smirnov test. Furthermore, no blunder errors were identified in the residual populations after applying the 3-sigma rule (Daniel and Tennant, 2001).

Results

Two independent statistical tests were developed using the accuracy estimates for the triangulations ($RMSE_p$, $RMSE_z$ and $RMSE_{3d}$ values obtained using CPs) as observed

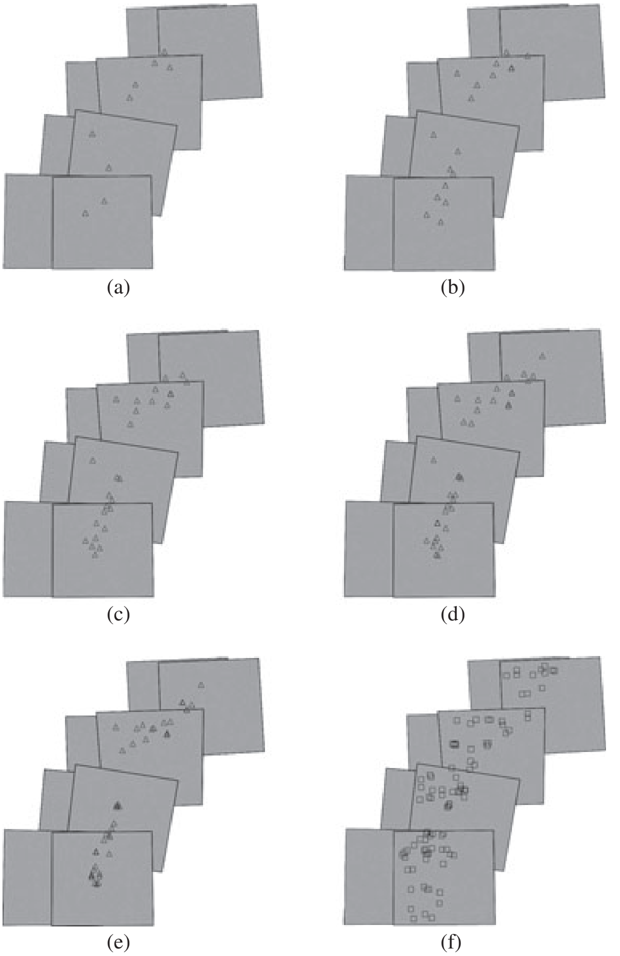

FIG. 5. Distribution of one of the three sets of GCPs and tie points used in the 1977 dataset: (a) 9 GCPs; (b) 18 GCPs; (c) 27 GCPs; (d) 36 GCPs; (e) 45 GCPs; (f) tie points.

variables. They were carried out from the 90 photogrammetric cases generated with both the 1956 and 1977 datasets, respectively. Within these statistical tests, the observed variance was partitioned into components due to the different sources of variation which had been considered. The two main factors analysed (namely, the number of GCPs and the method of self-calibration) were significant at the 95% level for both the 1956 and 1977 datasets. In both cases, the number of GCPs had the most significant repercussion in the ANOVA model, followed by the method of self-calibration. However, the interaction between the self-calibration method and the number of GCPs was not found to be significant, indicating that there are no statistical differences among the performance of the six calibration methods regarding the number of GCPs required to perform the triangulation.

Influence of the Number of GCPs on Triangulation Accuracy

1956 Dataset. Table II shows the global comparison of mean values of $RMSE_p$, $RMSE_z$ and $RMSE_{3d}$ from the 1956 and 1977 projects according to the number of GCPs and self-calibration methods. For example, 1·330 m is the $RMSE_p$ mean value obtained for all the photogrammetric projects carried out using the 1956 dataset and 45 GCPs for any self-calibration model, whereas 1·348 m is the $RMSE_p$ mean value for all the 1956 dataset's projects using the model of lens distortion for any number of GCPs. For the 1956 flight, the worst accuracies were generated using nine GCPs. In theory, of course, with more GCPs the accuracy should improve. Thus, the significant differences presented in Table II imply 27 GCPs would be optimal for this flight in terms of $RMSE_p$ and $RMSE_{3d}$ (for $RMSE_p$, 1·266 m using 27 GCPs and 1·290 m with 36 GCPs are the only values in this column which present significant differences with the mean value of 1·579m attained using 9 GCPs, because the 1·266 and 1·290 m values are the only ones without the letter "b", which accompanies the 9 GCPs value). However, 18 GCPs would be the ideal number of GCPs in the case of $RMSE_z$. Bearing in mind that GCPs were distributed across different numbers of stereopairs for each flight, it is perhaps prudent to refer to the ratio of the number of GCPs per stereopair. In this manner, the ideal ratio for the 1956 flight could range from 9 to 14 GCPs per stereopair.

1977 Dataset. In the case of the 1977 flight for $RMSE_p$, $RMSE_z$ and $RMSE_{3d}$, the best and significantly different ($p < 0{\cdot}05$) accuracies were generated when 27, 36 or 45 GCPs were used (Table II). Although the RMSE values for 36 and 45 GCPs were better than those attained using only 27 GCPs, no statistical differences were found. Thus, the optimal number of GCPs is around seven per stereopair for this flight.

TABLE II. Global comparison of mean values expressed in metres (m) of $RMSE_p$, $RMSE_z$ and $RMSE_{3d}$ from the 1956 and 1977 projects depending on the number of ground control points (GCPs) and self-calibration method.

	1956			*1977*		
	$RMSE_p$	*$RMSE_z$*	*$RMSE_{3d}$*	*$RMSE_p$*	*$RMSE_z$*	*$RMSE_{3d}$*
Number of GCPs						
45	$1{\cdot}330^{ab}$	$1{\cdot}438^{a}$	$1{\cdot}961^{ab}$	$0{\cdot}273^{a}$	$0{\cdot}377^{a}$	$0{\cdot}466^{a}$
36	$1{\cdot}290^{a}$	$1{\cdot}431^{a}$	$1{\cdot}929^{a}$	$0{\cdot}276^{a}$	$0{\cdot}371^{a}$	$0{\cdot}463^{a}$
27	$1{\cdot}266^{a}$	$1{\cdot}450^{a}$	$1{\cdot}928^{a}$	$0{\cdot}282^{a}$	$0{\cdot}405^{a}$	$0{\cdot}494^{a}$
18	$1{\cdot}344^{ab}$	$1{\cdot}555^{a}$	$2{\cdot}058^{ab}$	$0{\cdot}299^{b}$	$0{\cdot}478^{b}$	$0{\cdot}566^{b}$
9	$1{\cdot}579^{b}$	$1{\cdot}843^{b}$	$2{\cdot}438^{b}$	$0{\cdot}334^{c}$	$0{\cdot}618^{c}$	$0{\cdot}707^{c}$
Self-calibration method						
Lens distortion	$1{\cdot}348^{ab}$	$1{\cdot}415^{a}$	$1{\cdot}958^{a}$	$0{\cdot}287^{ab}$	$0{\cdot}445^{ab}$	$0{\cdot}530^{ab}$
Brown	$1{\cdot}312^{a}$	$1{\cdot}570^{b}$	$2{\cdot}049^{ab}$	$0{\cdot}277^{a}$	$0{\cdot}411^{a}$	$0{\cdot}496^{a}$
Jacobsen	$1{\cdot}379^{ab}$	$1{\cdot}562^{ab}$	$2{\cdot}087^{b}$	$0{\cdot}303^{c}$	$0{\cdot}458^{ab}$	$0{\cdot}551^{ab}$
Bauer	$1{\cdot}374^{ab}$	$1{\cdot}571^{b}$	$2{\cdot}091^{b}$	$0{\cdot}300^{c}$	$0{\cdot}451^{ab}$	$0{\cdot}544^{ab}$
Ebner	$1{\cdot}341^{a}$	$1{\cdot}600^{b}$	$2{\cdot}091^{b}$	$0{\cdot}297^{bc}$	$0{\cdot}433^{ab}$	$0{\cdot}528^{ab}$
NSC	$1{\cdot}418^{b}$	$1{\cdot}542^{ab}$	$2{\cdot}103^{b}$	$0{\cdot}294^{bc}$	$0{\cdot}501^{b}$	$0{\cdot}585^{b}$

RMSE values given in planimetry (p), height (z) and 3D (3d). Values in the same column followed by *different* superscript letters (a, b, c) indicate significant differences at a 95% significance level ($p < 0{\cdot}05$).

Influence of Self-Calibration Method on Triangulation Accuracy

The general results regarding the tested self-calibration models are also depicted in Table II. These results are provided in more detail in Tables III and IV for the 1956 and 1977 datasets, respectively, comparing the accuracies attained by applying the different self-calibration methods and varying the number of GCPs. Furthermore, the standard deviations corresponding to three repetitions are shown in parentheses as an indicator of the variability of the planimetric, vertical and three-dimensional RMSE mean values.

1956 Dataset. The results attained by the self-calibration models tested (Table II) for the 1956 archival flight were very changeable depending on the RMSE analysed. While the models of Brown and Ebner presented the best planimetric accuracies, the lens distortion model showed the best vertical results. In fact, when the number of GCPs was up to 27, only the lens distortion model could improve the vertical accuracies attained without self-calibration (Table III). It is noteworthy that using 27 GCPs (Table III), the $RMSE_p$ mean value for Brown's model was statistically better than those obtained using the lens distortion model or without self-calibration.

The best overall accuracy in terms of $RMSE_{3d}$ was achieved by means of the lens distortion model (Table II), although very closely followed (and without significant differences at $p < 0{\cdot}05$) by Brown's model. The models of Jacobsen, Bauer, Ebner and NSC presented values that were statistically significantly different to the lens distortion model. Regarding the detailed results for the number of GCPs used (Table III), the lens distortion model always attained the best accuracies, though being statistically significantly better against the models of Bauer, Jacobsen and Ebner only for the case of 36 GCPs. The standard deviations from the three repetitions, presented in Table III, were almost always higher for NSC than for any of the self-calibration models. That was true especially when the aerial triangulation was undertaken with a low number of GCPs. Hence, the results from the self-calibration methods can be deemed as more reliable.

The accuracy improvements achieved in the 1956 dataset using the lens distortion model compared with NSC were very dependent on the number of GCPs used. In addition, it was very dependent on the RMSE type being analysed (planimetric or vertical). Thus, using nine GCPs, $RMSE_p$ improved to approximately 0·15 m (a relative improvement of 9%), while $RMSE_z$ diminished to 0·22 m (11% degradation). On the other hand, when 27 GCPs were used, $RMSE_p$ was only improved to around 0·05 m (a relative improvement of approximately 3·8%), while $RMSE_z$ decreased to about 0·12 m (8·3% degradation).

1977 Dataset. For the 1977 flight, Brown's model could be considered as the optimal method overall, presenting significant differences ($p < 0{\cdot}05$) with respect to the NSC approach for planimetric, vertical and three-dimensional RMSE mean values (Table II). However, when the results were qualified by the number of GCPs (Table IV), Brown's model was only statistically better than using NSC in the case of 27 GCPs. The 1977 imagery had better radiometric quality and a larger scale than the 1956 dataset (Fig. 3), reducing the pointing error when measuring GCP positions in image space. Furthermore, the photography was acquired more recently and so the available GCP distribution was slightly better than for the 1956 dataset. In this sense, it is noteworthy that the standard deviations for the accuracy values in 1977 presented in Table IV were smaller than those for the 1956 flight.

Regarding accuracy improvements achieved in the 1977 dataset using Brown's model, $RMSE_p$ did not change when the nine GCPs scheme was applied, whereas $RMSE_z$ diminished to around 0·25 m (a 33% relative improvement). However, when 36 GCPs were

TABLE III. The 1956 archival flight.

Number of GCPs	Number of CPs	Accuracy (m)		Self-calibration method					
				NSC	*Lens*	*Bauer*	*Jacobsen*	*Ebner*	*Brown*
9	77 h 75 v	$RMSE_p$	Mean (SD)	1·647 (0·081)	1·499 (0·048)	1·598 (0·222)	1·613 (0·208)	1·593 (0·037)	1·526 (0·113)
		$RMSE_z$	Mean (SD)	1·987 (0·738)	1·769 (0·219)	1·926 (0·192)	1·882 (0·181)	1·748 (0·218)	1·748 (0·235)
		$RMSE_{3d}$	Mean (SD)	2·609 (0·573)	2·321 (0·188)	2·514 (0·019)	2·488 (0·040)	2·369 (0·136)	2·329 (0·114)
18	68 h 66 v	$RMSE_p$	Mean (SD)	1·372 (0·083)	1·309 (0·099)	1·363 (0·097)	1·383 (0·113)	1·339 (0·066)	1·300 (0·071)
		$RMSE_z$	Mean (SD)	1·585 (0·300)	1·433 (0·206)	1·568 (0·131)	1·555 (0·082)	1·622 (0·126)	1·567 (0·076)
		$RMSE_{3d}$	Mean (SD)	2·099 (0·281)	1·944 (0·186)	2·080 (0·110)	2·082 (0·105)	2·106 (0·056)	2·038 (0·033)
27	59 h 57 v	$RMSE_p$	Mean (SD)	1·346 (0·048)^{c}	1·295 (0·058)^{bc}	1·258 (0·032)^{ab}	1·254 (0·035)^{ab}	1·234 (0·040)^{ab}	1·209 (0·018)^{a}
		$RMSE_z$	Mean (SD)	1·390 (0·124)	1·274 (0·056)	1·468 (0·098)	1·469 (0·095)	1·582 (0·185)	1·513 (0·160)
		$RMSE_{3d}$	Mean (SD)	1·936 (0·108)	1·818 (0·037)	1·933 (0·091)	1·932 (0·087)	2·010 (0·132)	1·939 (0·117)
36	50 h 48 v	$RMSE_p$	Mean (SD)	1·351 (0·111)	1·309 (0·112)	1·300 (0·022)	1·296 (0·022)	1·250 (0·031)	1·236 (0·035)
		$RMSE_z$	Mean (SD)	1·374 (0·055)	1·279 (0·033)	1·459 (0·087)	1·464 (0·089)	1·527 (0·040)	1·484 (0·027)
		$RMSE_{3d}$	Mean (SD)	1·928 (0·101)^{ab}	1·832 (0·067)^{a}	1·955 (0·053)^{b}	1·957 (0·055)^{b}	1·973 (0·030)^{b}	1·932 (0·020)^{ab}
45	41 h 39 v	$RMSE_p$	Mean (SD)	1·372 (0·110)	1·327 (0·114)	1·353 (0·049)	1·350 (0·050)	1·291 (0·053)	1·289 (0·061)
		$RMSE_z$	Mean (SD)	1·375 (0·077)	1·321 (0·037)	1·434 (0·095)	1·440 (0·093)	1·524 (0·107)	1·536 (0·075)
		$RMSE_{3d}$	Mean (SD)	1·943 (0·115)	1·874 (0·088)	1·972 (0·077)	1·975 (0·079)	1·998 (0·086)	2·005 (0·084)

Mean values and standard deviations (in parentheses) of accuracy estimates for the triangulations ($RMSE_p$, $RMSE_z$ and $RMSE_{3d}$) measured at CPs (horizontal, h, and vertical, v) regarding the number of ground control points and the self-calibration method. Values in the same row followed by *different* superscript letters (a, b, c) indicate significant differences at a significance level $p < 0·05$. Values in rows without superscripts indicate no significant differences.

TABLE IV. The 1977 archival flight.

Number of GCPs	*Number of CPs*	*Accuracy (m)*		*Self-calibration method* *NSC*	*Lens*	*Bauer*	*Jacobsen*	*Ebner*	*Brown*
9	80 h 68 v	$RMSE_p$	Mean (SD)	0·328 (0·018)	0·334 (0·014)	0·333 (0·011)	0·339 (0·014)	0·338 (0·014)	0·331 (0·021)
		$RMSE_z$	Mean (SD)	0·778 (0·260)	0·570 (0·162)	0·587 (0·161)	0·609 (0·199)	0·638 (0·162)	0·524 (0·043)
		$RMSE_{3d}$	Mean (SD)	0·849 (0·235)	0·665 (0·135)	0·678 (0·138)	0·702 (0·176)	0·725 (0·140)	0·621 (0·034)
18	71 h 59 v	$RMSE_p$	Mean (SD)	0·297 (0·021)	0·293 (0·030)	0·309 (0·021)	0·312 (0·022)	0·304 (0·036)	0·281 (0·030)
		$RMSE_z$	Mean (SD)	0·563 (0·137)	0·465 (0·075)	0·469 (0·082)	0·472 (0·077)	0·468 (0·085)	0·432 (0·032)
		$RMSE_{3d}$	Mean (SD)	0·638 (0·127)	0·549 (0·079)	0·563 (0·070)	0·567 (0·063)	0·561 (0·070)	0·516 (0·040)
27	62 h 50 v	$RMSE_p$	Mean (SD)	0·286 (0·006)^{b}	0·278 (0·010)^{b}	0·290 (0·003)^{b}	0·292 (0·005)^{b}	0·285 (0·011)^{b}	0·261 (0·010)^{a}
		$RMSE_z$	Mean (SD)	0·446 (0·063)	0·415 (0·036)	0·410 (0·041)	0·417 (0·042)	0·377 (0·048)	0·367 (0·042)
		$RMSE_{3d}$	Mean (SD)	0·530 (0·057)^{b}	0·499 (0·035)^{ab}	0·503 (0·032)^{ab}	0·509 (0·033)^{ab}	0·474 (0·037)^{ab}	0·450 (0·036)^{a}
36	53 h 41 v	$RMSE_p$	Mean (SD)	0·281 (0·004)^{c}	0·268 (0·005)^{b}	0·285 (0·003)^{c}	0·287 (0·004)^{c}	0·280 (0·006)^{c}	0·258 (0·005)^{a}
		$RMSE_z$	Mean (SD)	0·372 (0·031)^{ab}	0·390 (0·020)^{b}	0·390 (0·020)^{b}	0·394 (0·022)^{b}	0·333 (0·029)^{a}	0·351 (0·028)^{ab}
		$RMSE_{3d}$	Mean (SD)	0·466 (0·027)^{ab}	0·473 (0·019)^{ab}	0·483 (0·015)^{b}	0·487 (0·017)^{b}	0·435 (0·023)^{a}	0·435 (0·025)^{a}
45	44 h 32 v	$RMSE_p$	Mean (SD)	0·277 (0·007)^{b}	0·262 (0·006)^{a}	0·284 (0·003)^{b}	0·284 (0·003)^{b}	0·277 (0·009)^{b}	0·253 (0·007)^{a}
		$RMSE_z$	Mean (SD)	0·346 (0·029)	0·385 (0·034)	0·400 (0·045)	0·400 (0·044)	0·347 (0·036)	0·382 (0·065)
		$RMSE_{3d}$	Mean (SD)	0·444 (0·022)	0·466 (0·031)	0·491 (0·039)	0·491 (0·037)	0·445 (0·033)	0·459 (0·058)

Mean values and standard deviations (in parentheses) of accuracy estimates for the triangulations ($RMSE_p$, $RMSE_z$ and $RMSE_{3d}$) measured at CPs (horizontal, h, and vertical, v) regarding the number of ground control points and the self-calibration method. Values in the same row followed by different superscript letters indicate significant differences at a significance level $p < 0·05$. Values in rows without superscripts do not present significant differences.

used, the $RMSE_p$ and $RMSE_z$ values only improved to around 0·02 m (a relative improvement of approximately 8% and 5·6%, respectively). As with the 1956 dataset, a relatively small accuracy improvement was attained by self-calibration when a high number of very accurate GCPs were used.

Discussion

Regarding the number of GCPs, in previous work Aguilar et al. (2009) attained similar accuracies when applying the self-calibration models included in the LPS software with 24 GCPs and 12 GCPs, using only one stereopair at a scale of 1:5000 for a flight taken in 2001 with a Zeiss RMK TOP 15 camera. On the other hand, Walstra (2006) estimated the interior orientation of five vertical archival photographs without a calibration certificate in a self-calibrating bundle adjustment using between four and nine GCPs per stereopair. In this case, the self-calibration was performed using GAP (General Adjustment Program) software developed by Chandler and Clark (1992). Considering these results, a suitable number of GCPs per stereopair to perform self-calibrating bundle adjustment could be placed at between six and nine. However, in the case of very old flights where the prints or negatives have not been appropriately conserved, are very hazy or are taken at small scales, it could be necessary to increase this ratio up to values closer to 14 GCPs per stereopair.

With regard to the self-calibration models tested, previous works carried out upon photogrammetric datasets acquired with film or digital cameras have reported the successful use of self-calibrating bundle adjustment methods with APs (see, for example, Ackermann, 1981; Cramer, 2009). According to Kraus (1997), the proper use of self-calibration might improve the accuracy of conventional aerial triangulation by 50%.

With regard to which self-calibration model is best applied, the recommendations from other work are very variable. For example, Ebner's model was presented as the best self-calibration approach for analogue photogrammetric datasets by both Cardenal et al. (2006) and Aguilar et al. (2009). Da Silva et al. (2008) identified the lens distortion model as the best self-calibration method included in the LPS software for correcting systematic errors in imagery taken with a Hasselblad digital camera. Alamús et al. (2006) considered four independent sets of Ebner's self-calibration parameters (one for each image quadrant) in the block adjustments to model Intergraph DMC systematic errors detected in adjustments. Moreover, working with a stereopair of conventional colour aerial photographs at a scale of 1:5000, but scanned from negatives and using 24 GCPs, Aguilar et al. (2005) reported $RMSE_{3d}$ values of 0·252 m after the self-calibrating bundle adjustment was carried out using a low-cost close-range software package. In this case, the principal point coordinates, affine image parameters (A, B) to correct for scale difference and non-perpendicularity of the x and y image coordinates, radial lens distortion parameters (k_1, k_2) and decentring lens distortion parameters (p_1, p_2) were calculated. Working on the same stereopair and with the same aforementioned number of GCPs, Aguilar et al. (2009) attained $RMSE_{3d}$ values of 0·153 and 0·57 m using the models of Ebner and Brown, respectively.

All the works mentioned above point to the underlying hypothesis constituting the basis of the current work, namely, that self-calibration techniques should be able to remove, at least partially, the presence of systematic errors. This was found to be true in many cases where certain conditions were fulfilled, such as: no correlation among APs; good distribution of GCPs in three dimensions; highly redundant photographic coverage; low pointing errors in image space (pre-marked points); preferably highly convergent photography; and, maybe the most relevant constraint, where systematic deformations were similar for all images in the block. In other words, the APs are treated as block invariant. Unfortunately, this supposition is only correct in cases of homogeneous projects (such as one camera, one roll of film, same flight direction and so on) where any significant random errors due to poor conservation of the images are absent. Indeed, the assumption of systematic image errors which are constant for a whole set of photography cannot always account for the total error budget, which would also include correlation and variation of image deformations within a series of photographs. As already demonstrated by other authors, sometimes it may even be recommended to apply alternative APs to different strips or groups of photographs belonging to a certain area. In this sense, it is necessary to clarify that any extrapolation of the results from a locally computed self-calibration bundle adjustment to those areas outside the area bounded by the GCPs (even in the same stereoscopic model) should definitely be avoided. In this project, it should be taken into account that the quality of the self-calibration will be compromised by the poor planimetric and vertical distribution of GCPs due to the age of the imagery (and hence the difficulty in surveying proper GCPs), by the typically low relief of coastal areas (small vertical range) and by the presence of the sea occupying a high percentage of some photographs. However, all these characteristics are very common in archival photogrammetric imagery over coastal areas and, therefore, the approach is justified when working under real operational conditions.

Examining the 1956 dataset investigated here, it is noteworthy that $RMSE_{3d}$ attained using 9 GCPs and without self-calibration was about 3·7 times higher than the GSD, whereas using the lens distortion model with 27 GCPs this value decreased to 2·6 times the GSD. These low accuracies might be expected since the photography was very old and in poor condition. Furthermore, the photography had a low resolution and poor radiometric quality, which made it difficult to precisely measure the corresponding GCPs in the image space (see Figs. 3 and 4). Subsequently, the GCP pointing error arising from this dataset may be deemed as excessively large, thereby contributing to somehow masking the possible improvements derived from the application of the tested self-calibration models. In summary, there is an underlying masking effect due to higher degree sources of error as compared to the sort of systematic errors that can be properly modelled by self-calibration, which is very typical for archival photogrammetric imagery. Besides, the distribution of GCPs and tie points could be considered quite poor. As a reference, it should be noted that Cardenal et al. (2006) reported an accuracy of 3·86 m (measured as $RMSE_{3d}$ on CPs) working with imagery from the "American flight".

In the case of the 1977 dataset, using nine GCPs and without self-calibration, the $RMSE_{3d}$ was around 3·1 times higher than the image GSD. On the other hand, with 36 GCPs and applying Brown's model, the $RMSE_{3d}$ value decreased to 1·6 times the image GSD. Walstra et al. (2007) reported $RMSE_{3d}$ accuracies within the range of 1·31 m (4·8 GSD) and 0·63 m (2·3 GSD) for archival datasets acquired in 1971 and 1995, respectively, displaying a GSD similar to that of the 1977 flight investigated here.

Finally, a further reason which may explain why it is very difficult to highlight a single self-calibration method as optimal for all cases encountered in this work, could be related to the fact that the blocks are well-controlled. In this case, the standard bundle block adjustment (NSC case) could already be expected to compensate well for systematic errors. In that case, APs would only produce, at best, a relatively moderate improvement on the accuracy of adjusted coordinates. Given the low standard deviations computed when working with more than 18 GCPs (1956) or even only 9 GCPs in the case of the 1977 data, both blocks could be deemed as relatively well controlled.

Conclusions

This paper has addressed the important issue of adopting self-calibrating bundle adjustment models, as included in commercial software, to try to improve the accuracy of results attained from the photogrammetric triangulation of historic aerial imagery taken at different scales and times on a specific pilot area. The underlying hypothesis of this work proposes that self-calibration with APs might model the difference between the theoretical perspective geometry and the real image geometry for archival aerial photography and so remove, at least partially, the presence of systematic errors. The research has involved extensive fieldwork that provided a large number of very accurate ground points (GCPs and CPs). The use of accuracy estimations based on a large number of CPs makes the findings of the study reliable. Moreover, repetitively undertaking each experiment has allowed the realisation of a full statistical analysis which enables the following conclusions to be drawn.

(1) *Number of GCPs used in triangulation*. The recommended number of accurate GCPs for performing a self-calibrating bundle adjustment with archival photography could be placed within the range of six to nine GCPs per stereopair. However, when working with very old photography at small scales it could be necessary to increase this number to somewhere between 12 and 16 GCPs per stereopair.

(2) *Self-calibrating bundle adjustment*. The best three-dimensional accuracies were achieved for the 1956 dataset using the lens distortion model, although this was very closely followed by Brown's model (without statistically significant differences). For the 1977 dataset, Brown's model was found to be the best self-calibration method. The recommendation should always be to test other models since each flight can present systematic errors of a different nature. In fact, the scale and special characteristics of each archival photogrammetric flight are, probably, the most important factor affecting the choice of self-calibration model. Therefore, every archival dataset should be treated in an independent and empirical way depending on its own particular characteristics. Furthermore, it may sometimes be recommended to apply alternative APs to different strips or groups of photographs belonging to a certain spatial area. In this sense, it is necessary to clarify that any extrapolation of the results from a locally computed self-calibration bundle adjustment to those areas outside the area delimited by the GCPs (even within the same stereoscopic model) should definitely be avoided.

(3) *Accuracy improvement by applying self-calibration models*. Low relative three-dimensional accuracy improvements were achieved using self-calibration models when a high number of very accurate GCPs were available. $RMSE_p$ and $RMSE_z$ improved by around 4% to 8% with respect to NSC for the two archival datasets. However, the accuracy improvement for $RMSE_p$ ranged from 0% to 9% when using only nine GCPs, whereas $RMSE_z$ diminished by between 11% and 33%. Hence, self-calibration techniques included in LPS software would be especially interesting when the number of GCPs is small. There are two main reasons which could explain the relatively poor performance of the self-calibration applied in this work. Firstly, there is an underlying masking effect due to higher degree sources of error, as compared to the sort of systematic errors that can be properly modelled by self-calibration, which is very typical for archival photogrammetric imagery. The magnitude of such non-systematic errors could be much higher than systematic errors which can be solved by self-calibration. Thus, the results are more heavily influenced by the number of GCPs used in the bundle adjustment than the self-calibration model employed. Furthermore, the APs are computed as an average for the whole block, but each photograph could have its own systematic errors which would explain the reason why it is very difficult to point out a method as

optimal for all the cases examined. The second reason relates to the fact that the blocks were relatively well controlled. In these cases, the standard bundle adjustment of the block (NSC case) usually compensates well for systematic errors and APs would only produce, at best, a moderate improvement on the accuracy of adjusted coordinates.

As further research, it would be useful to compare the optimised accuracies achieved here using a high number of very accurate GCPs with the results obtained by other approaches such as those based on surface matching. Such approaches avoid the costly and time-consuming necessity of collecting GCPs, which may be almost impossible to identify in archival photography.

ACKNOWLEDGEMENTS

This work was supported by the Andalusia Regional Government, Spain, through Excellence Research Project RNM-3575. The authors also appreciate the support from the Spanish Ministry for Science and Innovation under Grant Reference CTM2010-16573. These two research projects were co-financed by the European Union under the European Regional Development Fund (ERDF).

REFERENCES

ACKERMANN, F., 1981. Block adjustment with additional parameters. *Photogrammetria*, 36(6): 217–227.

AGUILAR, F. J., AGUILAR, M. A., FERNÁNDEZ, I., NEGREIROS, J. G., DELGADO, J. and PÉREZ, J. L., 2012. A new two-step robust surface matching approach for three-dimensional georeferencing of historical digital elevation models. *IEEE Geoscience and Remote Sensing Letters*, 9(4): 589–593.

AGUILAR, M. A., AGUILAR, F. J. and AGÜERA, F., 2005. Mapping small areas using a low-cost close range photogrammetric software package with aerial photography. *Photogrammetric Record*, 20(112): 335–350.

AGUILAR, M. A., AGUILAR, F. J. and NEGREIROS, J. G., 2009. Self-calibration methods for using historical aerial photographs with photogrammetric purposes. *Anales de Ingeniería Gráfica*, 21: 33–40.

AKCA, D., 2010. Co-registration of surfaces by 3D least squares matching. *Photogrammetric Engineering & Remote Sensing*, 76(3): 307–318.

ALAMÚS, R., KORNUS, W. and TALAYA, J., 2006. Studies on DMC geometry. *ISPRS Journal of Photogrammetry and Remote Sensing*, 60(6): 375–386.

AMIRI PARIAN, J. and GRUEN, A., 2010. Sensor modeling, self-calibration and accuracy testing of panoramic cameras and laser scanners. *ISPRS Journal of Photogrammetry and Remote Sensing*, 65(1): 60–76.

BAUER, H. and MÜLLER, J., 1972. Height accuracy of blocks and bundle block adjustment with additional parameters. *International Archives of Photogrammetry*, Commission III, Ottawa, Canada. 9 pages.

CARDENAL, J., DELGADO, J., MATA, E., GONZÁLEZ, A. and OLAGUE, I., 2006. Use of historical flight for landslide monitoring. *7th International Symposium on Spatial Accuracy Assessment in Natural Resources and Environmental Sciences*, Lisbon, Portugal. 129–138.

CHADWICK, J., DORSCH, S., GLENN, N., THACKRAY, G. and SHILLING, K., 2005. Application of multi-temporal high-resolution imagery and GPS in a study of the motion of a canyon rim landslide. *ISPRS Journal of Photogrammetry and Remote Sensing*, 59(4): 212–221.

CHANDLER, J. H. and COOPER, M. A. R., 1989. The extraction of positional data from historical photographs and their application to geomorphology. *Photogrammetric Record*, 13(73): 69–78.

CHANDLER, J. H. and CLARK, J. S., 1992. The archival photogrammetric technique: further application and development. *Photogrammetric Record*, 14(80): 241–247.

CRAMER, M., 2009. *Digital Camera Calibration*, Official Publication No. 55. European Spatial Data Research (EuroSDR), Frankfurt am Main, Germany. 262 pages.

DA SILVA, R., GARCÍA, A. M., GALO, M., KIYOSHI, J. and CESAR, R., 2008. Fototriangulação com parâmetros adicionais para câmaras digitais: uma avaliação experimental. *Boletim de Ciências Geodésicas*, 14(4): 571–587.

DANIEL, C. and TENNANT, K., 2001. DEM quality assessment. *Chapter 12 in Digital Elevation Model Technologies and Applications: The DEM Users Manual* (Ed. D. F. Maune). American Society for Photogrammetry and Remote Sensing, Bethesda, Maryland, USA. 539 pages: 395–440.

EBNER, H., 1976. Self calibrating block adjustment. *Bildmessung und Luftbildwesen*, 44(4): 128–139.
FRASER, C. S., 1997. Digital camera self-calibration. *ISPRS Journal of Photogrammetry and Remote Sensing*, 52(4): 149–159.
GRÜN, A., 1978. Experiences with self-calibrating bundle adjustment. *American Congress on Surveying and Mapping/American Society of Photogrammetry (ACSM-ASP)*, Washington, DC, USA. 23 pages.
JAMES, T. D., MURRAY, T., BARRAND, N. E. and BARR, S. L., 2006. Extracting photogrammetric ground control from lidar DEMs for change detection. *Photogrammetric Record*, 21(116): 312–328.
KLEIN, H., 1979. New results of bundle block adjustments with additional parameters. *37th Photogrammetric Week*, Stuttgart, Germany. *Schriftenreihe* 6(1980): 13–30.
KRAUS, K., 1997. *Photogrammetry. Volume 2. Advanced Methods and Applications*. Fourth edition. Dümmler, Bonn, Germany. 466 pages.
LANE, S. N., 2000. The measurement of river channel morphology using digital photogrammetry. *Photogrammetric Record*, 16(96): 937–961.
LEICA GEOSYSTEMS, 2006. Leica Photogrammetry Suite Project Manager. Leica Geosystems Geospatial Imaging, LLC, Norcross, Georgia, USA. 434 pages. http://gis.ess.washington.edu/data/erdas_pdfs/LPS_PM.pdf [Accessed: 22nd September 2011].
LI, Z., XU, Z., CEN, M. and DING, X., 2001. Robust surface matching for automated detection of local deformations using least-median-of-squares estimator. *Photogrammetric Engineering & Remote Sensing*, 67(11): 1283–1292.
LICHTI, D. D., 2010. Terrestrial laser scanner self-calibration: correlation sources and their mitigation. *ISPRS Journal of Photogrammetry and Remote Sensing*, 65(1): 93–102.
MARZOLFF, I. and POESEN, J., 2009. The potential of 3D gully monitoring with GIS using high-resolution aerial photography and a digital photogrammetry system. *Geomorphology*, 111(1–2): 48–60.
MILLER, P., MILLS, J., EDWARDS, S., BRYAN, P., MARSH, S., MITCHELL, H. and HOBBS, P., 2008. A robust surface matching technique for coastal geohazard assessment and management. *ISPRS Journal of Photogrammetry and Remote Sensing*, 63(5): 529–542.
MILLS, J. P., BUCKLEY, S. J. and MITCHELL, H. L., 2003. Synergistic fusion of GPS and photogrammetrically generated elevation models. *Photogrammetric Engineering & Remote Sensing*, 69(4): 341–349.
MILLS, J. P., BUCKLEY, S. J., MITCHELL, H. L., CLARKE, P. J. and EDWARDS, S. J., 2005. A geomatics data integration technique for coastal change monitoring. *Earth Surface Processes and Landforms*, 30(6): 651–664.
PROKEŠOVÁ, R., KARDOŠ, M. and MEDVEĎOVÁ, A., 2010. Landslide dynamics from high-resolution aerial photographs: a case study from the Western Carpathians, Slovakia. *Geomorphology*, 115(1–2): 90–101.
QUIRÓS, F. and FERNÁNDEZ, F., 1997. El vuelo fotográfico de la "Serie A". *Ería: Revista cuatrimestral de Geografía*, 43: 190–198.
SCHIEFER, E. and GILBERT, R., 2007. Reconstructing morphometric change in a proglacial landscape using historical aerial photography and automated DEM generation. *Geomorphology*, 88(1–2): 167–178.
SNEDECOR, G. W. and COCHRAN, W. G., 1980. *Statistical Methods*. Seventh edition. Iowa State University Press, Ames, Iowa, USA. 507 pages.
VÉGA, C. and ST-ONGE, B., 2008. Height growth reconstruction of a boreal forest canopy over a period of 58 years using a combination of photogrammetric and lidar models. *Remote Sensing of Environment*, 112(4): 1784–1794.
WALSTRA, J., 2006. *Historical aerial photographs and digital photogrammetry for landslide assessment*. Ph.D. thesis, Loughborough University, Loughborough, UK. 228 pages.
WALSTRA, J., DIXON, N. and CHANDLER, J. H., 2007. Historical aerial photographs for landslide assessment: two case histories. *Quarterly Journal of Engineering Geology and Hydrogeology*, 40(4): 315–332.
ZANUTTA, A., BALDI, P., BITELLI, G., CARDINALI, M. and CARRARA, A., 2006. Qualitative and quantitative photogrammetric techniques for multi-temporal landslide analysis. *Annals of Geophysics*, 49(4–5): 1067–1080.

Résumé

L'utilisation de photographies d'archive pour une exploitation photogrammétrique se heurte souvent à un manque de données concernant les instruments de prise de vue aérienne employés, à des difficultés d'identification de points d'appui dans les clichés, et à une mauvaise conservation des photographies. Lorsque les paramètres d'étalonnage de l'instrument sont inconnus, ils doivent pouvoir être estimés par auto-étalonnage au moyen d'une compensation par faisceaux. Plusieurs modèles d'étalonnage proposés par le logiciel LPS

(Leica Photogrammetry Suite) ont été testés sur deux jeux de données d'archive, acquis en 1956 et 1977 sur le même site. Il s'avère que la précision de la triangulation dépend étroitement de la méthode d'auto-étalonnage et du nombre de points d'appui utilisés. En utilisant entre six et neuf points par couple stéréoscopique, l'auto-étalonnage par compensation de faisceaux améliore légèrement, quoique pas toujours de manière significative, le potentiel photogrammétrique des photographies aériennes d'archive. Toutefois, la mise en œuvre de l'auto-étalonnage ne garantit pas l'amélioration des résultats lorsque les images ont été mal conservées. Les résultats obtenus avec de telles données dépendent de nombreuses variables locales qui ne peuvent pas être extrapolées à d'autres sites y compris pour un même instrument, car chaque jeu de données est unique et peut présenter des erreurs systématiques qui lui sont propres.

Zusammenfassung

Zur Verwendung von historischen Bildern für die Photogrammetrie fehlen oft Daten der Luftbildkammern. Dazu kann es schwierig sein, Passpunkte in den Bildern zu identifizieren und die Bilder können Schäden durch ungeeignete Lagerung aufweisen. Falls die Kalibrierparameter unbekannt sind, sollten sie durch eine Selbstkalibrierung im Rahmen einer Bündelausgleichung bestimmt werden. Hierzu sind in der Leica Photogrammetry Suite Software mehrere Kalibriermodelle verfügbar. Diese wurden an zwei Datensätzen von Archivbildern, die in den Jahren 1956 und 1977 aufgenommen worden waren, erprobt. Die Genauigkeit der Triangulation dieser Datensätze hing signifikant von der Methode der Selbstkalibrierung und der Anzahl der Passpunkte ab. Bei einer Passpunktzahl von sechs bis neun Punkten pro Stereobildpaar, konnten die untersuchten Verfahren der Bündelausgleichung mit Selbstkalibrierung die photogrammetrischen Möglichkeiten der historischen Luftbilder verbessern, allerdings nicht immer. Somit kann bei schlecht konservierten Archivbildern nicht unbedingt mit einer Verbesserung der Ergebnisse gerechnet werden. Die Ergebnisse solcher Datensätze hängen sehr stark von zahlreichen lokalen Variablen ab, die nicht auf andere Gebiete mit der gleichen Kamera übertragen werden können, da jeder Datensatz einzigartig ist und somit auch systematische Fehler unterschiedlicher Art aufweisen kann.

Resumen

El uso en fotogrametría de fotografías de archivo o históricas a menudo conlleva una carencia de información relativa a las cámaras aéreas empleadas, dificultades en la identificación de puntos de control sobre las fotos y una inapropiada conservación de los fotogramas. Cuando los parámetros de calibración de la cámara son desconocidos, el ajuste de bloque con auto calibración podría ser usado. Varios modelos de auto calibración disponibles en el paquete fotogramétrico Leica Photogrammetry Suite han sido probados en dos vuelos fotogramétricos históricos, tomados en 1956 y 1977, sobre la misma área de estudio. La precisión de la triangulación dependió de forma significativa del método de auto calibración y del número de puntos de control empleados; de hecho, cuando se usaron entre 6 y 9 puntos de control por estéreo par, el empleo de auto calibración mostró ligeras, aunque no siempre estadísticamente significativas, mejoras en los resultados obtenidos a partir de vuelos fotogramétricos de archivo. De ese modo, el uso de auto calibración no garantiza la mejora de las precisiones obtenidas en la triangulación de imágenes aéreas mal conservadas. Los resultados en estos casos dependen de numerosas variables locales que no pueden ser extrapoladas a otras áreas tomadas con la misma cámara, ya que cada vuelo fotogramétrico es único y puede presentar errores sistemáticos de diferente naturaleza.